

QC  
801  
.U6  
E2  
no.26  
c.2

NOAA Technical Memorandum EDIS 26



---

GATE RADAR RAINFALL PROCESSING SYSTEM

Washington, D.C.  
May 1979

---

**noaa**

NATIONAL OCEANIC AND  
ATMOSPHERIC ADMINISTRATION

Environmental Data and  
Information Service

NOAA TECHNICAL MEMORANDUMS

Environmental Data and Information Service Series

Environmental Data and Information Service (EDIS) is responsible for storing, retrieving, and publishing NOAA data and for developing systems to process and present NOAA data in the most statistical form. These data, which relate to the solid earth, ocean, atmosphere, space, are the basic input in scientific and engineering studies having broad application in agriculture, commerce, defense, and industry.

The NOAA Technical Memorandum EDIS facilitates rapid distribution of studies and reports which may be preliminary in nature and which may be published formally elsewhere at a later date. Publications 1 and 2 are in a former series of Weather Bureau Technical Notes (TN); publications 3 to 17 are in a former series of ESSA Technical Memorandums designated as Environmental Data Service Technical Memorandums (EDSTM). Beginning with 18, publications are now part of the NOAA Technical Memorandum EDIS series and are designated as either EDS or EDIS.

Publications listed below are available from the National Technical Information Service, U.S. Department of Commerce, Sills Bldg., 5285 Port Royal Road, Springfield, VA 22161. Price: Varies for paper copy; \$3.00 microfiche. Order by accession number shown in parentheses at end of each entry.

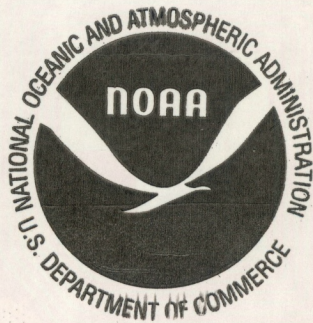
Weather Bureau Technical Notes

- TN 33 Part 1: Weather and Disease. H. E. Landsberg. Part 2: Solar Radiation and Skin Cancer  
EDS 1 Deaths. G. D. Brinckerhoff. February 1966. (PB-169-813)
- TN 43 A Bibliography of Meso- and Micro-Environmental Instrumentation. John F. Griffiths and M.  
EDS 2 Joan Griffiths, July 1966. (PB-173-088)

ESSA Technical Memorandums

- EDSTM 3 Climatological Aspects of Air Pollution in West Virginia. Robert O. Weedfall, January 1967.  
(PB-176-905)
- EDSTM 4 Estimates of Winds at Constant Heights Generated From Winds Observed at Constant Pressure  
Surfaces. H. L. Crutcher, H. B. Harshbarger, R. L. Durham, F. T. Quinlan, J. D. Matthews, and  
W. B. Tschiffely, February 1967. (PB-174-499)
- EDSTM 5 Synoptic Aspects of Mortality: A Case Study. Dennis M. Driscoll, February 1967. (PB-174-  
500)
- EDSTM 6 A Technique for Determination of a Climatology of High Altitude Balloon Trajectories. Frank  
T. Quinlan and Lee R. Hoxit. October 1968. (PB-180-200)
- EDSTM 7 Minimum Temperature Patterns Over New York State on Two Winter Nights. A. Boyd Pack, Febru-  
ary 1969. (PB-183-398)
- EDSTM 8 Coastal Weather and Marine Data Summary for Gulf of Alaska, Cape Spencer Westward to Kodiak  
Island. Harold W. Searby, May 1969. (PB-184-784)
- EDSTM 9 A Bibliography of Weather and Architecture. John F. Griffiths and M. Joan Griffiths, April  
1969. (PB-184-969)
- EDSTM 10 A Note on Climatology of Thailand and Southeast Asia. H. L. Crutcher, S. Bintasant Nash, and  
D. K. Kropp, May 1969. (PB-187-569)
- EDSTM 11 Meteorological Drought in West Virginia. Robert O. Weedfall, September 1969. (PB-187-474)
- EDSTM 12 Snowfall, Snowfall Frequencies, and Snow Cover Data for New England. R. E. Lautzenheiser,  
December 1969. (PB-194-221)
- EDSTM 13 Applications of Air Mass Classifications to West Virginia Climatology. Robert O. Weedfall,  
January 1970. (PB-191-966)
- EDSTM 14 Georgia Tropical Cyclones and Their Effect on the State. Horace S. Carter, January 1970.  
(PB-190-768)

(Continued on inside back cover)



PC  
801  
46E2  
no. 26  
C. 2

NOAA Technical Memorandum EDIS 26

GATE RADAR RAINFALL PROCESSING SYSTEM

Vernon L. Patterson, Michael D. Hudlow,  
Peter J. Pytlowany, Frank P. Richards, and  
John D. Hoff

Washington, D.C.  
May 1979

SILVER SPRING  
CENTER  
  
JUN 22 1979  
  
N.O.A.A.  
U. S. Dept. of Commerce

UNITED STATES  
DEPARTMENT OF COMMERCE  
Juanita M. Kreps, Secretary

NATIONAL OCEANIC AND  
ATMOSPHERIC ADMINISTRATION  
Richard A. Frank, Administrator

Environmental Data and  
Information Service  
Thomas S. Austin, Director



# CONTENTS

	<u>Page</u>
Abstract . . . . .	1
1. Introduction . . . . .	1
2. Input data . . . . .	4
3. Conversion program . . . . .	7
3.1 Input cleanup . . . . .	7
3.2 Conversion of reflectivity values to rainfall rates . . . . .	8
3.3 Objective analysis "center-fill" routine . . . . .	8
3.4 Atmospheric attenuation corrections . . . . .	12
3.5 Wet-radome attenuation corrections for <u>Oceanographer</u> radar . . . . .	14
3.6 Intervening rainfall attenuation corrections . . . . .	15
3.7 Beam-filling correction for <u>Researcher</u> radar . . . . .	19
3.8 Systematic biases . . . . .	20
3.9 Data navigation . . . . .	20
3.10 Quality control . . . . .	21
4. Preprocessing of <u>Gilliss</u> and <u>Quadra</u> radar data . . . . .	22
4.1 Adjustments to reflectivity arrays . . . . .	22
4.2 Specific corrective actions . . . . .	22
4.2.1 <u>Gilliss</u> editing procedures . . . . .	22
4.2.2 <u>Quadra</u> editing procedures . . . . .	24
4.3 Evaluation of preprocessing procedures . . . . .	25
5. Merge programs . . . . .	25
6. Integration program . . . . .	29
7. Concluding remarks . . . . .	30
Acknowledgments . . . . .	32
References . . . . .	33

## FIGURES

		<u>Page</u>
1	B-scale and master arrays and the location of the C-band radars used in the rainfall derivations for Phases I and II of GATE . . . . .	2
2	B-scale and master arrays and the location of the C-band radars used in the rainfall derivations for Phase III of GATE . . . . .	3
3	Data flow and summary of processing steps leading to instantaneous, refined rainfall estimates from individual C-band radars . . . . .	5
4	Flow diagram of the merge and integration steps of the precipitation processing system . . . . .	6
5	Network of data bins used with the objective analysis model to estimate the rainfall rates at the radar origin and in the four data bins surrounding the origin . . . . .	10
6	Sequence in which intervening rainfall corrections were applied to the first 64 Cartesian data bins . . . . .	16
7	Schematic illustration of the segmentation of a path, when applying eq. (8), from the radar origin (O) to a point (d) at the center of a Cartesian data bin for which the intervening rain attenuation is being calculated . . . . .	17
8	Areal coverage within the master array by the <u>Oceanographer</u> and <u>Researcher</u> radars during Phases I and II . . . . .	26
9	Areal coverage within the master array by the four C-band radars during Phase III . . . . .	28
10	Sample map of hourly rainfall accumulations within the master array for the hour ending 1800 GMT on September 2 . . . . .	31

## TABLES

1	Two-way attenuation in rainfall rate units (dBR) by water vapor and oxygen for C-band radiation propagating in a mean GATE atmosphere (antenna elevation of 0.75° assumed) . . . . .	13
2	Two-way attenuation in rainfall rate units (dBR) at 30°C caused by water film buildup on the <u>Oceanographer's</u> spherical radome versus rainfall rate . . . . .	15
3	Reflectivity adjustments for <u>Gilliss</u> and <u>Quadra</u> radar data . . . . .	23

TABLES (continued)

Page

4 Number of scans for which specific corrective actions were made to the Gilliss and Quadra data . . . . . 24

# GATE RADAR RAINFALL PROCESSING SYSTEM

Vernon L. Patterson, Michael D. Hudlow, Peter J. Pytlowany,  
Frank P. Richards, and John D. Hoff

Center for Environmental Assessment Services<sup>1</sup>  
Environmental Data and Information Service, NOAA, Washington, D.C.

ABSTRACT. As part of the GARP Atlantic Tropical Experiment (GATE), quantitative precipitation observations, covering an array of ships centered at 8°30' N. latitude and 23°30' W. longitude, were made during the summer of 1974 using four C-band digital radars complemented by shipboard rain gages. This report describes the system of programs that was developed to derive rainfall estimates from the individual radars, to correct these estimates for such effects as atmospheric attenuation, to navigate and merge the estimates from the individual radars within a master array, and to integrate the instantaneous estimates for hourly periods. The resultant data, consisting of hourly rainfall amounts for a Cartesian network of 4-km square data bins, were archived both on magnetic tapes and microfilm. A sample rainfall map is included. The quality of the data is excellent and the problems identified in the use of the data have been very few and minor, leading us to believe that the precipitation processing system was successful and that all crucial refinements were made to improve the quality of the data.

## 1. INTRODUCTION

During the GARP<sup>2</sup> Atlantic Tropical Experiment (GATE), quantitative precipitation observations, for an array centered at 8°30' N. latitude and 23°30'W. longitude, were made using four C-band digital radars complemented by shipboard rain gages. High-quality rainfall estimates were derived for a master array somewhat larger than the GATE B-scale array (figs. 1 and 2). The data collection and validation of methods used to

---

<sup>1</sup>Formerly the Center for Experiment Design and Data Analysis.

<sup>2</sup>Global Atmospheric Research Program.

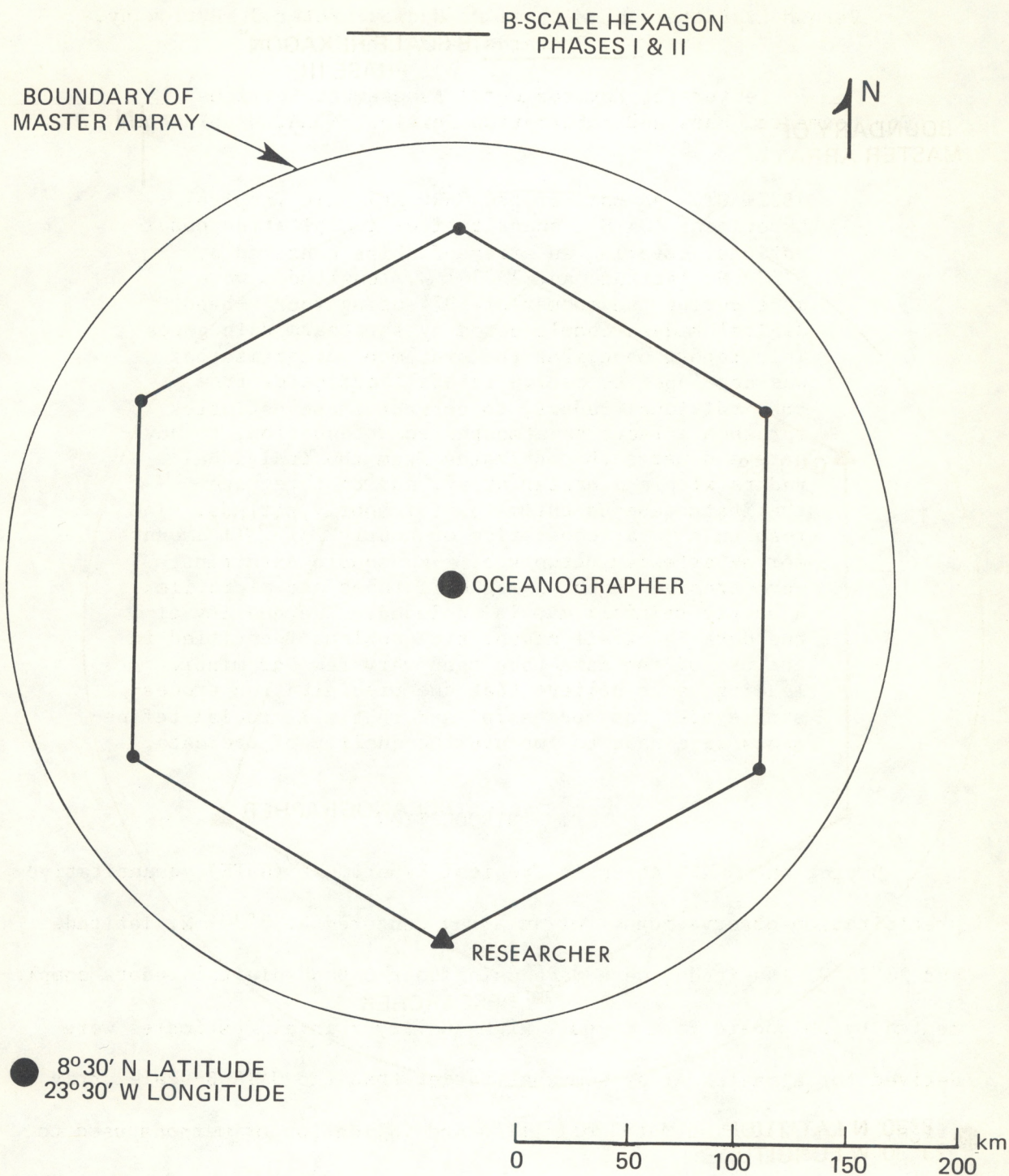


Figure 1. B-scale and master arrays and the location of the C-band radars used in the rainfall derivations for Phases I and II of GATE.



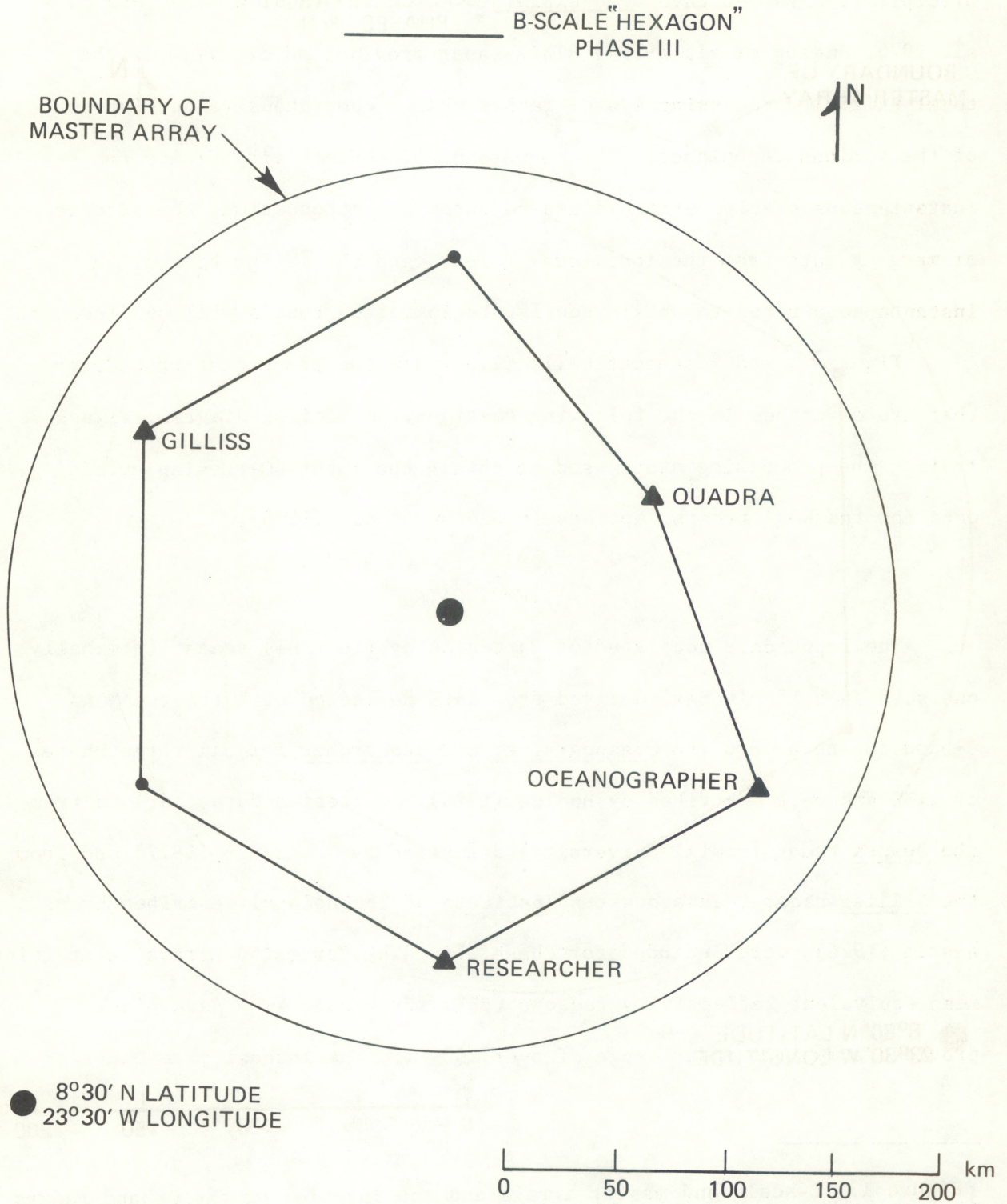


Figure 2. B-scale and master arrays and the location of the C-band radars used in the rainfall derivations for Phase III of GATE.

convert the radar reflectivities from individual radars to quantitative precipitation values have been explained elsewhere (Hudlow 1975, Hudlow et al. 1976, Hudlow et al. 1979). This paper provides an overview of the total rainfall processing system rather than a comprehensive development of the various techniques. The conversion of reflectivity fields to instantaneous precipitation values adjusted for attenuation, the process of merging data from the individual radars, and the integration of the instantaneous rates to obtain hourly precipitation totals will be discussed.

Figures 3 and 4 schematically illustrate the processing procedures that are described in the following sections. A similar diagram, illustrating the processing steps used to obtain the input (Cartesian hybrid) data for the NOAA radars, appears in Hudlow et al. (1976).

## 2. INPUT DATA

The input data consisted of Cartesian hybrid (PPI) scans<sup>3</sup> (nominally one scan each 15 minutes) derived from data collected with the two NOAA C-band radars aboard the Oceanographer and Researcher for all three Phases of GATE and were described by Hudlow (1976). Cartesian data, derived from the Quadra radar (McGill University) described by G. Austin (1977) and from the Gilliss radar (Massachusetts Institute of Technology) described by P. Austin (1976), were included for Phase III. The Cartesian arrays, containing mean equivalent reflectivity factors (dBZ) for 4-km x 4-km data bins, provided a maximum radar range of over 200 km. The intensity resolution

---

<sup>3</sup>A scan in the context of this report is 360° of data arranged in a plan-position-indicator (PPI) format.

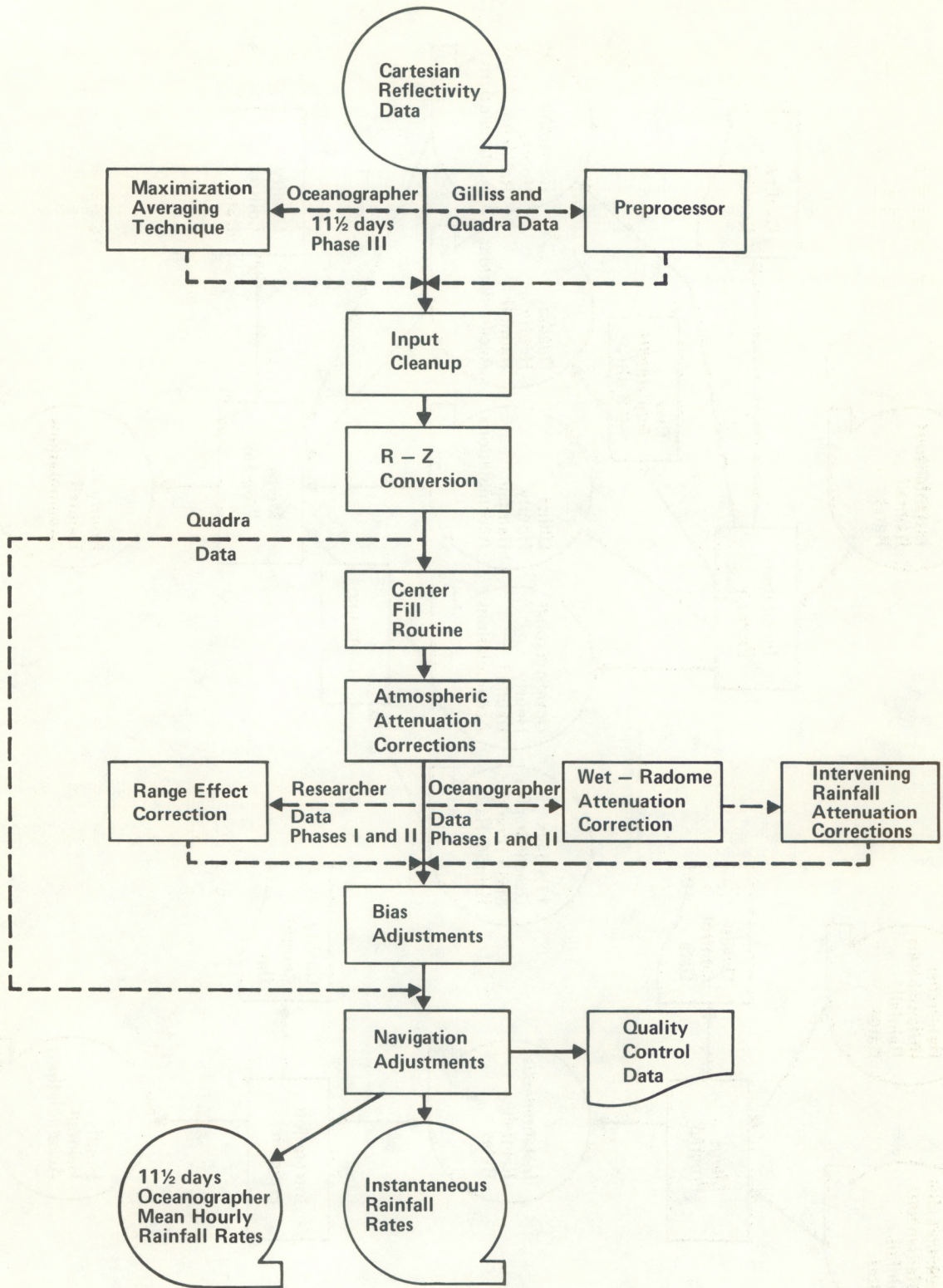
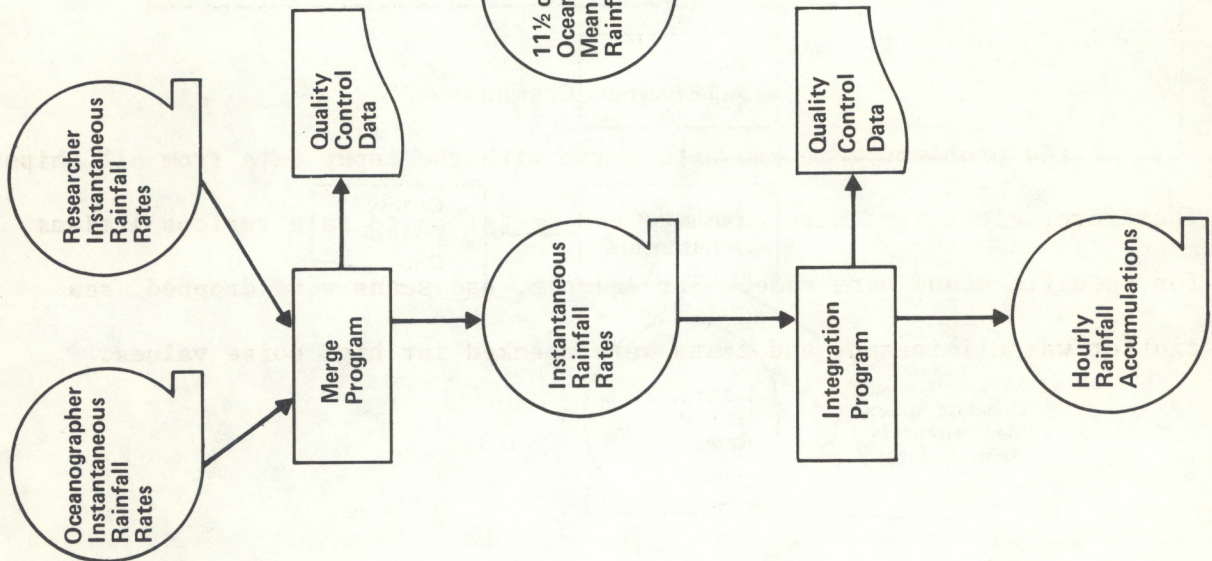


Figure 3. Data flow and summary of processing steps leading to instantaneous, refined rainfall estimates from individual C-band radars.

PHASES I AND II



PHASE III

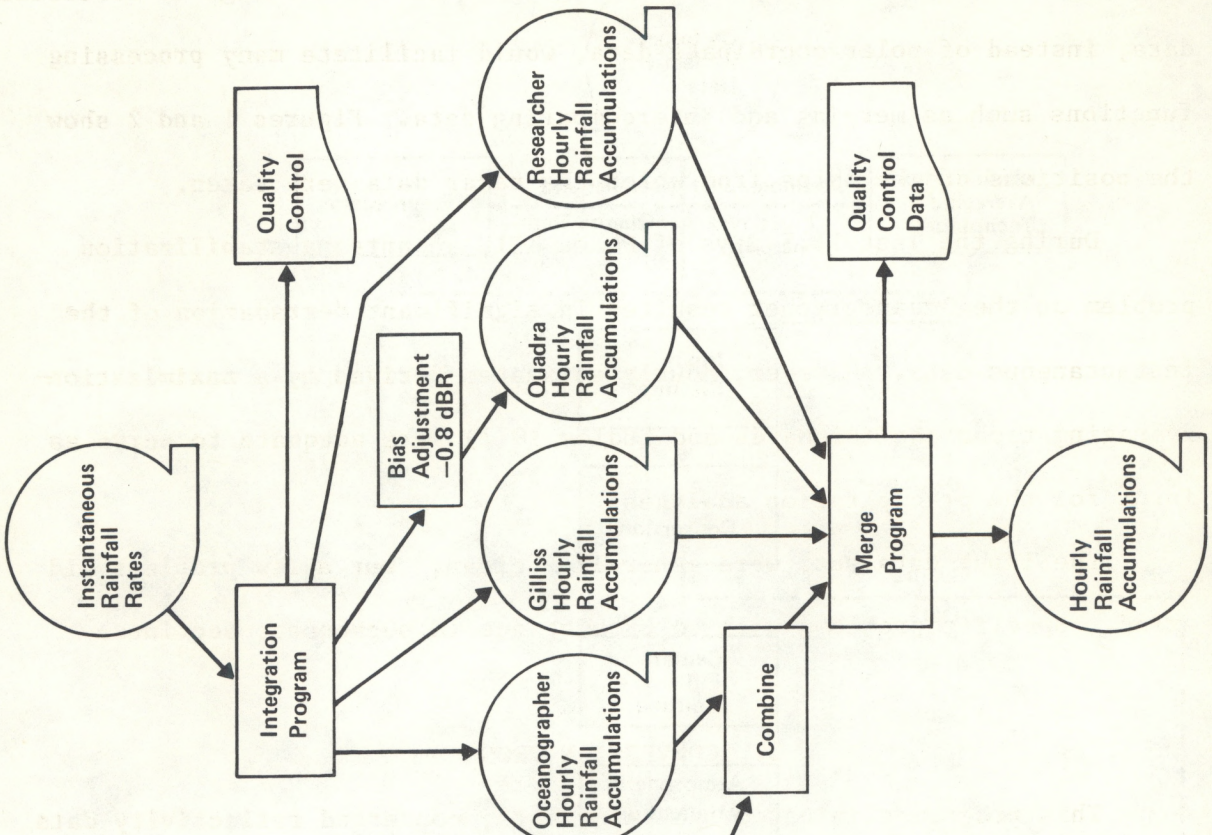


Figure 4. Flow diagram of the merge and integration steps of the precipitation processing system.

was 1 dBZ. NOAA and the universities agreed that the exchange of Cartesian data, instead of polar coordinate data, would facilitate many processing functions such as merging and intercomparing data. Figures 1 and 2 show the positions of the ships from which the radar data were taken.

During the last 11.5 days of Phase III, an antenna stabilization problem on the Oceanographer resulted in significant degradation of the instantaneous data. However, hourly estimates derived by a maximization-averaging technique (Richards and Hudlow 1977) were adequate to serve as input for the precipitation analyses.

The input data sets were generally "clean," but a few problems did exist. Specific problems will be brought out in subsequent sections.

### 3. CONVERSION PROGRAM

This program eliminated bad input data, converted reflectivity data (dBZ) to rainfall rates (dBR), interpolated for missing data, applied corrections, and checked the validity of the rainfall rate estimates.

#### 3.1 Input Cleanup

A few problems were known to exist with the input data from all ships. Therefore, microfilms were examined and decisions to take various actions for specific scans were made. For example, bad scans were dropped, sea clutter was eliminated, and scans were checked for high noise values.

### 3.2 Conversion of Reflectivity Values to Rainfall Rates

The conversion of reflectivity<sup>4</sup> to rainfall was based on the following relationship:

$$R = 0.013Z_e^{0.8}, \quad (1)$$

where R is rainfall rate in mm hr<sup>-1</sup> and Z<sub>e</sub> is the equivalent reflectivity factor in mm<sup>6</sup> m<sup>-3</sup>. Equation (1) is a mean GATE relationship based on the pooling of the disdrometer data from shipboard and airborne platforms (Austin et al. 1976). From eq. (1), we obtain

$$\text{dBR} = 0.8 \text{ dBZ} + 10 \log_{10} 0.013, \quad (2)$$

where dBR and dBZ are rainfall rates and reflectivities expressed in decibels referenced to 1 mm hr<sup>-1</sup> and 1 mm<sup>6</sup> m<sup>-3</sup> for rainfall rate and reflectivity, respectively. As shown by Hudlow and Arkell (1978), variability of the Z-R relationship is not a significant source of error for the time and spatial scales being considered for GATE atmospheric budget studies (> 3 hr, > 4000 km<sup>2</sup>). However, errors introduced by variabilities in the Z-R relationship may become significant for smaller scales.

### 3.3 Objective Analysis "Center-Fill" Routine

To minimize the areal extent of the sea clutter, digital hybrid scans were composited for the three U.S. radars using annuli from scans

---

<sup>4</sup>The terms reflectivity and reflectivity factor are used interchangeably in this report.

collected at the three lowest antenna tilt angles (Hudlow et al. 1976, Richards and Hudlow 1977, P. Austin 1976). The tilt angles and range extents for the three annuli used in the construction of the hybrids were approximately  $0.5^\circ$ ,  $r > 32$  km;  $2.0^\circ$ ,  $16$  km  $< r \leq 32$  km; and  $4.0^\circ$ ,  $4$  km  $< r \leq 16$  km. Hybrid scans were not constructed for the Quadra since data were not available for ranges inside 16 km (G. Austin 1977). Significant sea clutter rarely, if ever, existed in the Quadra base-tilt data at ranges exceeding 16 km.

When all three of the lowest tilt scans were available for the construction of hybrids, sea clutter contamination was eliminated from all except the four closest Cartesian data bins surrounding the origin. In addition to the intense sea clutter signals that persisted, "main-bang" spillover and clutter from the ship's superstructure also contributed to contamination of these four closest data bins. To obtain instantaneous radar-rainfall estimates for the four inner Cartesian bins and at the radar origin, an objective analysis model was developed.

The "center-fill" objective analysis model is similar to that described by Hudlow et al. (1976). In the present model, however, the time dependency terms were dropped from the polynomial interpolator because subsequent testing of the original model showed that 15-min samples were generally too far apart to adequately define the time history of the rainfall over very small areas. The analysis region for the spatial interpolator remains the same as that used in the earlier study and is shown in figure 5.

With the omission of all time terms, the polynomial model given by Hudlow et al. (1976) reduces to a quadratic expression equivalent to the one investigated by Greene (1971) for rectifying radar fields from polar to

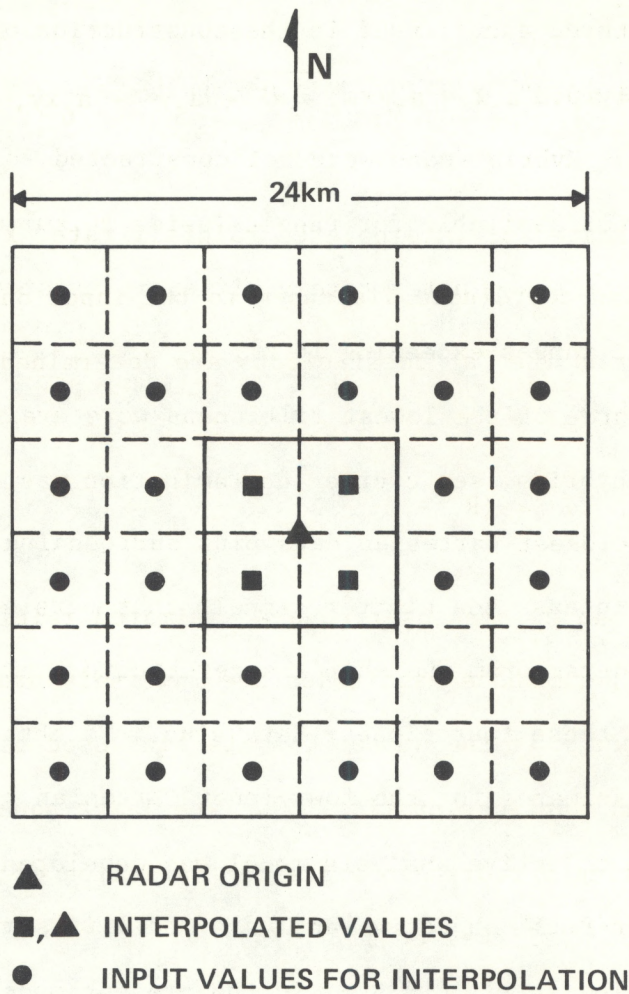


Figure 5. Network of data bins used with the objective analysis model to estimate the rainfall rates at the radar origin and in the four data bins surrounding the origin.



Cartesian coordinates. The quadratic function for this study can be written as

$$\hat{R} = a_1 + a_2x + a_3y + a_4x^2 + a_5y^2 + a_6xy, \quad (3)$$

where  $\hat{R}$  is the estimated or interpolated rainfall rate,  $x$  and  $y$  are normalized Cartesian coordinate distances to the input data bins from the radar origin, and the "a" coefficients are determined so that

$$\sum_{i=1}^N w_i (R_i - \hat{R}_i)^2 \quad (4)$$

is minimized.  $R_i$  and  $\hat{R}_i$  are observed and estimated rainfall rates, respectively,  $w_i$  are weights whose magnitudes are inversely proportional to distance from the origin, and  $N$  is the number of data bins used to fit eq. (3);  $N$  equals 32 for our application (fig. 5). The least-squares solution is accomplished by using a reorthogonalization variation of the classical Gram-Schmidt method (Jallickee et al. 1974).

The weights,  $w_i$ , are given by

$$w_i = (d_i^{-\beta}) / \sum_{i=1}^{32} (d_i^{-\beta}), \quad (5)$$

where  $d_i$  are the normalized distances from the radar origin to the centers of the input data bins. For the rainfall processing system, a  $\beta$  of 4.0 was empirically determined to provide "optimal" interpolations. The large  $\beta$  coefficient is consistent with the results of Hudlow et al. (1976) that show the average correlation radius (lag where the autocorrelation coeffi-

cient decreases to  $e^{-1}$ ) to be only 4-8 km for GATE convective rainfall at an instant in time. Exclusion of the time-dependency terms from the polynomial model resulted in the selection of a considerably larger  $\beta$  than in the 1976 study. That study, using test regions where interpolated values were compared to observed values, pointed out a weakness of the model. When there were large intensities and steep gradients somewhere within a 24-km x 24-km analysis region but only light or no rain at the point to be estimated, the model estimates tended to "overshoot" the observed values. The severity of this problem is significantly reduced by fitting the fields in dBR units, thereby compressing the dynamic range of the input data. However, the dBR fit tends to underestimate any large rain rates occurring at the points being interpolated. In practice, we found that a good compromise consisted of using the dBR fit for  $\hat{dBR} \leq 1.0$  and the R fit for  $\hat{dBR} > 1.0$ , where  $\hat{dBR}$  is an interpolated estimate from the dBR fit. A threshold of 1.0 dBR corresponds to  $1.25 \text{ mm hr}^{-1}$ .

### 3.4 Atmospheric Attenuation Corrections

An attenuation model derived by Hudlow et al. (1979), based on a mean GATE atmosphere and an antenna elevation angle of  $0.75^\circ$ , was used to apply atmospheric attenuation corrections to the U.S. radar data. The corrections were given by the following polynomial:

$$A = 2.115 \times 10^{-2}r - 4.340 \times 10^{-5}r^2 - 7.945 \times 10^{-8}r^3 + 2.595 \times 10^{-10}r^4, \quad (6)$$

where A is the total two-way attenuation (dBR) by water vapor and oxygen and r is the slant range (km). These corrections were applied only to the

Gilliss, Oceanographer, and Researcher data. Atmospheric attenuation corrections were applied electronically to the Quadra data before they were recorded. The Quadra corrections were based on a midlatitude, mean atmospheric sounding and are somewhat smaller than the corrections applied to the other three radars. Table 1 gives examples of atmospheric attenuation amounts from eq. (6) for several ranges.

Table 1.--Two-way attenuation in rainfall rate units (dBR) by water vapor and oxygen for C-band radiation propagating in a mean GATE atmosphere (antenna elevation of  $0.75^\circ$  assumed)

Range (km)	H <sub>2</sub> O	O <sub>2</sub>	H <sub>2</sub> O + O <sub>2</sub>
10	0.1	0.1	0.2
30	0.25	0.35	0.6
50	0.4	0.55	0.95
70	0.5	0.7	1.2
100	0.65	1.0	1.65
150	0.75	1.3	2.05
200	0.8	1.5	2.3

### 3.5 Wet-Radome Attenuation Corrections for Oceanographer Radar

Generally, unless a radome skin is a very efficient water repellent (hydrophobic) substance, water film buildup in moderate to heavy rainfall will cause some attenuation in the C band. Because the Oceanographer radar data were fundamental to the accuracy of the B-scale rainfall derivations during Phases I and II (fig. 1), corrections for wet-radome attenuation were applied. (Wet-radome corrections were not added to any other data.) Thirty-minute accumulations from rain gages were used to estimate rainfall rates at the time of the scans, and attenuation values were estimated from water film thicknesses given by an analytical model presented by Gibble (1964). (See also Hudlow et al. 1976 and Hudlow et al. 1979.) Empirical analyses, using the GATE Oceanographer radar and rain-gage data, indicated that Gibble's model gave overestimates of attenuation for the Oceanographer's radome (Hudlow et al. 1979). Accordingly, the two-way attenuation estimates, obtained with Gibble's model, were reduced by 1.3 dBR. The revised amounts for various rainfall rates are given in table 2. Since heavy precipitation occurred infrequently at the Oceanographer, wet-radome attenuation was seldom a significant factor. For example, the estimates of wet-radome attenuation were less than 1.0 dBR for more than 98 percent of the hours during Phases I and II (Hudlow et al. 1979). The maximum correction of 4.7 dBR for wet-radome attenuation was applied at 2145 GMT on July 7.

Table 2.--Two-way attenuation in rainfall rate units (dBR) at 30°C caused by water film buildup on the Oceanographer's spherical radome vs rainfall rate

Rainfall rate (mm/hr)	Attenuation
2.5	0.0
5	0.4
10	1.0
20	1.8
40	2.75
80	4.0

### 3.6 Intervening Rainfall Attenuation Corrections

Geotis (1977) derived a relationship between attenuation coefficient and reflectivity using electromagnetic theory and drop-size measurements made on the Gilliss during GATE. The relationship for two-way attenuation expressed in terms of rainfall rate using eq. (1) is

$$\gamma \approx 1.6 \times 10^{-3} R^{1.1}, \quad (7)$$

where  $\gamma$  is the attenuation coefficient (dBR km<sup>-1</sup>) and R is the rainfall rate (mm hr<sup>-1</sup>). The following computational form was used to apply the corrections:

$$dBR_c = dBR_{uc} + (1.6 \times 10^{-3}) \sum_{i=1}^{N_r} \{10^{[.1(dBR_i)_c/10]}\} \Delta r, \quad (8)$$

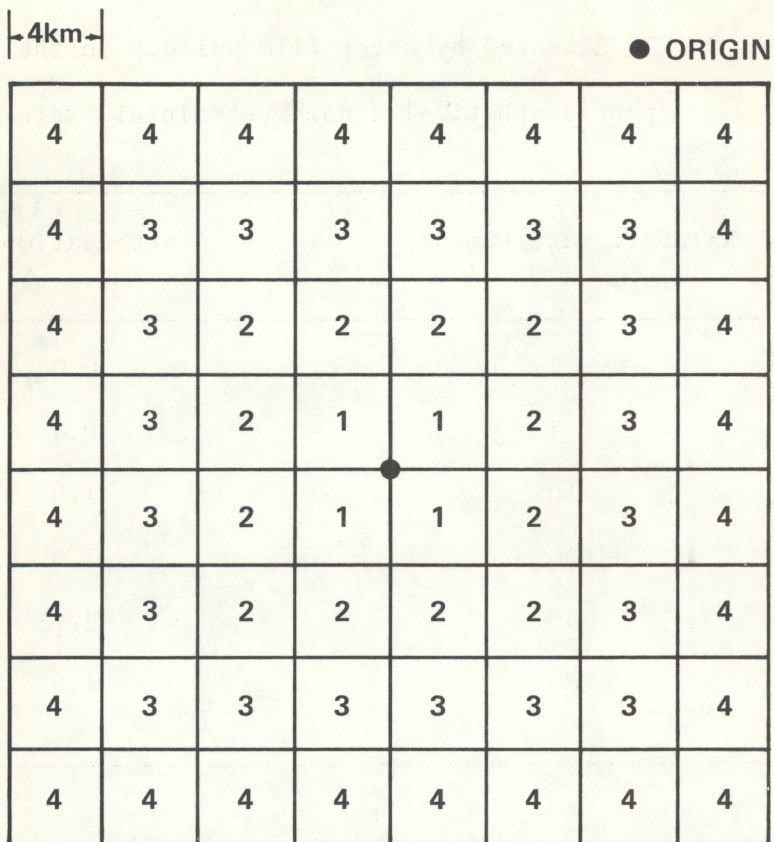


Figure 6. Sequence in which intervening rainfall corrections were applied to the first 64 Cartesian data bins.

where  $dBR_c$  and  $dBR_{uc}$  are the corrected and uncorrected values expressed in decibels referenced to  $1 \text{ mm hr}^{-1}$  at some range ( $r$ ),  $N_r$  is the number of finite path segments of length  $\Delta r$  (km) between the radar origin and the value being corrected, and  $(dBR_i)_c$  is the corrected rain value in decibels for the  $i^{\text{th}}$  segment. Intervening rainfall corrections were first calculated for the four data bins closest to the origin, then the next 12 closest bins, then the next 20 closest bins, etc., until all data were corrected. Figure 6 shows the sequence in which the first 64 bins were corrected. Figure 7 illustrates the segmentation of the path from the origin (0) to the bin centered at  $d$ . Rainfall rates were calculated for the points

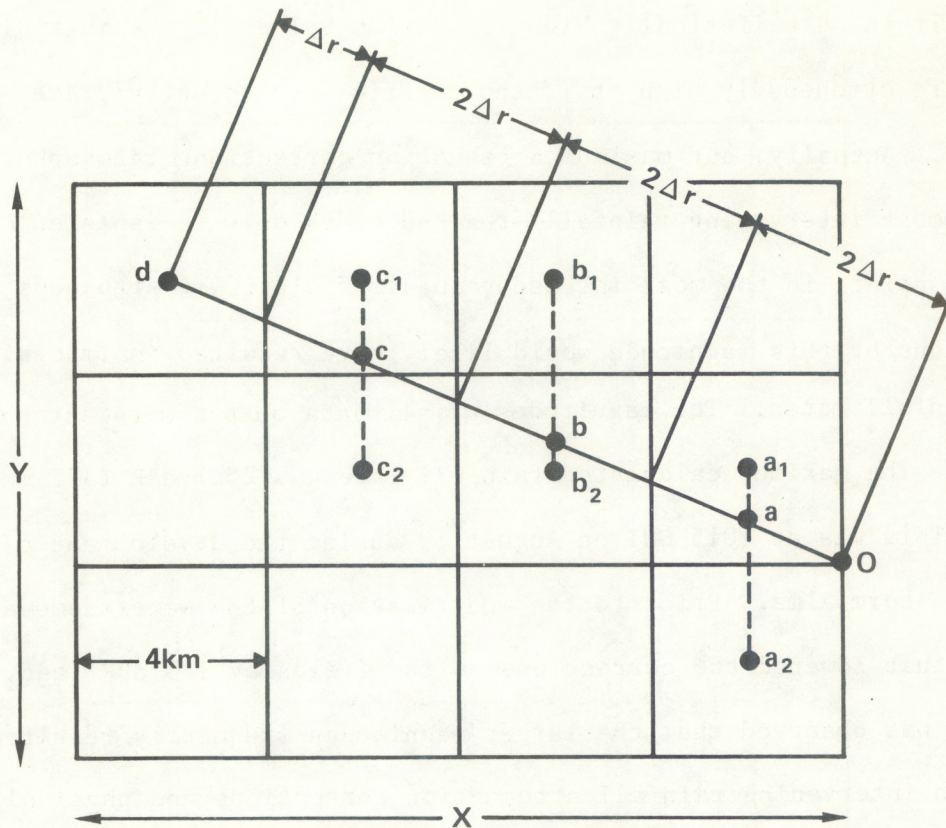


Figure 7. Schematic illustration of the segmentation of a path, when applying eq. (8), from the radar origin (0) to a point (d) at the center of a Cartesian data bin for which the intervening rain attenuation is being calculated.

a, b, and c by linearly interpolating between the rainfall rates for the bins centered at  $a_1$  and  $a_2$ ,  $b_1$  and  $b_2$ , and  $c_1$  and  $c_2$ . The calculated rates at the points a, b, and c were assumed to be representative for the segments of length  $2\Delta r$ . The rainfall rate for the bin centered at d was assumed to be representative for the segment of length  $\Delta r$ .

Geotis (1975) found that there was a practical upper limit, "certainly less than 10 dB" (8 dBR), to the magnitude of corrections for intervening rainfall attenuation which could be automatically applied. Our attenuation correction procedure for intervening rainfall uses a cumulative logarithmic function (eq. 8). This procedure will give unstable solutions

and result in unrealistically high correction values if the initial data fields are erroneously high or if the coefficients in eq. (7) are significantly in error. Actually, our maximum attenuation corrections (atmospheric + wet radome + intervening rainfall) reached 8 dBR only in isolated cases at a few points in the most intense rainfall fields. If erroneous, corrections of this magnitude would likely have resulted in impossibly high rainfall rates. The magnitudes of all data output were automatically checked. The maximum calculated rainfall rate was 25.7 dBR (372 mm  $\text{hr}^{-1}$ ). This was at 1015 GMT on August 10 during the development of Tropical Storm Alma. Prior to the modification of the wet-radome attenuation routine that lowered the corrections to the fields by 1.3 dBR (sec. 3.5), it was observed that the larger magnitudes frequently resulted in very high intervening rainfall attenuation corrections and physically unrealistic rainfall rates. The fact that the application of the final routine did not result in unstable or physically unrealistic solutions is an indication of the validity of the input data and the conversion process.

The maximum attenuation correction from intervening rainfall only, applied to any data bin, was less than 5 dBR for all scans. Large corrections were necessary for only a small percentage of the scans, and significant corrections were confined to only a few data bins within a scan (Hudlow et al. 1979). For about 90 percent of the hours during Phases I and II, the maximum correction(s) applied during the hour to any data bin(s) was less than 2 dBR.

Attenuation corrections for intervening rainfall, as well as for wet-radome attenuation, were applied only to Oceanographer data for Phases I and II. These refinements were necessary because the Oceanographer's



central position during Phases I and II (fig. 1) made the quality of these data essential to the accuracy of the B-scale rainfall estimates. Rainfall attenuation corrections were not considered significant for Phase III because data were merged from more radars, each of which viewed the precipitation lying in the interior of the array from different directions (fig. 2). Also, the merging process was somewhat different for Phase III than for Phases I and II (sec. 5). Furthermore, as was discussed above, significant attenuation of C-band radar signals by rainfall during GATE occurred infrequently. Hildebrand (1978) finds C-band signals are seriously attenuated above 50 dBZ. However, the 4-km x 4-km reflectivities rarely exceeded 50 dBZ during GATE (Hudlow and Arkell 1978), and intense rain cores exceeding 50 dBZ had very small horizontal dimensions (Geotis 1977).

### 3.7 Beam Filling Correction for Researcher Radar

Intercomparisons of Oceanographer and Researcher data indicated that the magnitudes of the Researcher data were comparatively low at the greater ranges (Hudlow et al. 1979). This is consistent with the fact that the beam width for the Researcher radar is  $0.5^\circ$  larger than that of the Oceanographer ( $2.0^\circ$  versus  $1.5^\circ$ ). During Phases I and II only, the following adjustment factor was added to the Researcher dBR values to improve the merged rainfall estimates for ranges greater than 150 km:

$$B = 0.022 r - 3.27 \quad , \quad (9)$$

where  $r$  is the range (km) and  $B$  is the additive correction factor (dBR). The maximum correction was 2.36 dBR at 256 km. Actually, the intercomparison analysis by Hudlow et al. (1979) indicated that larger average corrections

might have been warranted; however, eq. (9) was used because it gave conservative corrections that probably never led to overestimates for R.

### 3.8 Systematic Biases

Intercomparisons of the radar rainfall estimates between radars and with rain-gage data (Hudlow et al. 1979) indicated that overall bias adjustments were necessary. These adjustments, for the various radar data sets used in the derivation of the hourly rainfall maps, were Oceanographer = +2.2 dBR, Researcher = +1.8 dBR, and Gilliss = -0.8 dBR for ranges less than 25 km and +0.8 dBR for ranges greater than 25 km. The instantaneous Quadra data were adjusted by a variable amount dependent upon the magnitude of the reflectivities (sec. 4). Also, the Quadra hourly rainfall estimates were adjusted by an additional -0.8 dBR before they were merged with data from the other C-band radars (secs. 5 and 6).

### 3.9 Data Navigation

The radar input data were Cartesian arrays comprised of 4-km x 4-km data bins centered relative to the ships' positions. Earth positions for the U.S. ships were obtained from a high-resolution navigational file (Seguin and Crayton 1975) and from a similar file for the Quadra provided by Geoffrey Austin, McGill University. The input reflectivity data were first converted to rainfall rates and then placed in a Cartesian master array comprised of 100 x 100, 4-km square bins centered at 8° 30' N. latitude and 23° 30' W. longitude (figs. 1 and 2). The bins in the corners of the array, beyond 204 km from the center, were set to a missing value. Data were placed in the master array to the nearest bin, meaning that the placement was within one-half data bin from the location

indicated by the navigation data. Any attempt to make finer adjustments would have required interpolation between data bins with resultant smearing.

### 3.10 Quality Control

To determine if there were any unknown problems with the input data, to avoid the inadvertent exclusion of data, and to reduce the probability of errors being introduced by the processing, various information (either printed or placed on microfilm) was routinely examined (fig. 3). The date/time groups for all scans were checked. Wet-radome and intervening rainfall attenuation corrections were examined for continuity and for consistency with the input data. Provision was made to print precipitation rates that were higher than likely to be encountered in valid data (sec. 3.6). Sample scans were plotted and validated against the input data, and microfilm graphics of all precipitation maps were inspected for time and space continuity on a film viewer in the time-lapse mode.

## 4. PREPROCESSING OF GILLISS AND QUADRA RADAR DATA

Preliminary assessments of the Cartesian reflectivity data from the Gilliss and Quadra radars indicated the need for an independent editing and analysis package to resolve isolated problems and apply reflectivity adjustments. Therefore, unique but similar procedures were implemented to preprocess the Gilliss and Quadra data, enabling coherent merging of all data sets into the master array.

### 4.1 Adjustments to Reflectivity Arrays

Systematic adjustments to the dBZ fields for each ship were made using the transformations shown in table 3. These bias adjustments reflect the results from a comprehensive intercomparison study using the shipboard rain-gage and quantitative radar data (Hudlow et al. 1979).

### 4.2 Specific Corrective Actions

The preprocessing programs for the Gilliss and Quadra data sets were designed to take certain corrective actions when flags relating to particular arrays were set. An action common to both consisted of deletion of "noisy" or otherwise bad scans. The nature and frequency of these actions are summarized in table 4.

#### 4.2.1 Gilliss Editing Procedures

Four corrective actions were occasionally required; the first three were applied with comparable frequency (table 4): 1) deletion of the more questionable scan whenever two scans existed for the same 15-min observation time, 2) maximization of relectivities over two scans when significant data degradation resulted from inaccurate antenna stabilization,

Table 3. Reflectivity adjustments for Gilliss and Quadra radar data

Original	<u>Gilliss</u> dBZ		<u>Quadra</u> dBZ	
	r < 25 km	Adjusted r > 25 km	Original**	Adjusted
0	0	0	<15***	0
1	0	2	16	16
2	1	3	17	17
3	2	4	19	19
4	3	5	22	22
.	.	.	24	24
.	.	.	26	25
.	.	.	28	26
.	.	.	30	27.5
.	.	.	32	29
48	47	49	34	30.5
49	48	50	36	33
50	48	50	38	35.5
51	49	51	40	38
52	50	52	42	41
53*	48	50	44	44
54	48	50	46	46
.	.	.	48	48
.	.	.	50	50
.	.	.	52	52
64	48	50	54	54

\* Original values equal to or greater than 53 dBZ were considered fictitiously high because of an integrator shift problem and were therefore lowered to a probable upper limit.

\*\* Because of a transcription error, the original translation table provided by McGill University gave 2 dBZ higher original values than those shown here. The additional 2 dBZ difference is not included because it resulted from an inadvertent error and not a system calibration bias.

\*\*\* Many of the reflectivity values at these levels are contaminated by radio frequency (RF) interference and were therefore set to 0 dBZ.

and 3) "zeroing" of the 24-km x 24-km grid array centered at the radar origin for those times when little or no precipitation was detected there and it was apparent that, because of missing data at the higher tilt settings, the hybrid compositing procedure had been unable to remove sea clutter contamination. The fourth action, based on visual inspection of individual scans, was applied only once throughout the processing and consisted of specifying an upper threshold level or cap. Above this level, the prevalence of noise in echo-void regions required setting these values to zero dBZ.

#### 4.2.2 Quadra Editing Procedures

Actions required for specific Quadra arrays included 1) deletion of those scans in which extensive data degradation by noise was evident and 2) thresholding the reflectivity values so that, for values below a certain specified minimum, an assignment of zero dBZ was made. The latter action was needed to eliminate radio frequency (RF) interference signals that persisted above the standard threshold level of 15 dBZ (table 3).

Table 4. Number of scans for which specific corrective actions were made to the Gilliss and Quadra data

	Deletion	Maximization	Clutter elimination	"Capping"	Raised threshold
<u>Gilliss</u>	45	96	43	1	N/A
<u>Quadra</u>	100	N/A	N/A	N/A	100

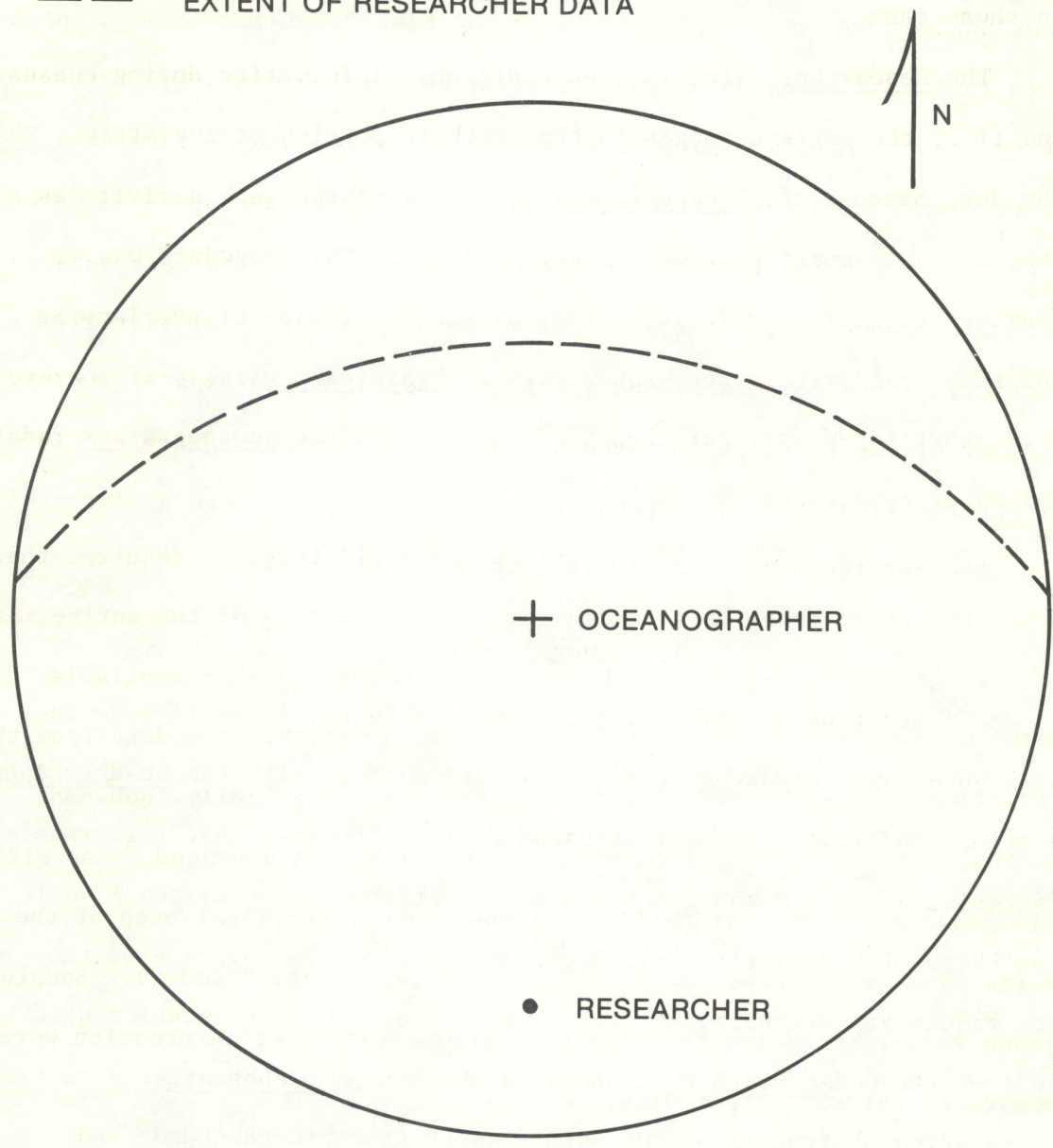
### 4.3 Evaluation of Preprocessing Procedures

As part of a quality assessment of the systematic and scan-specific actions applied during the preprocessing and also to discern range-dependent effects in the adjusted data, range statistics were obtained by first deriving average rainfall parameters over 20-km x 30° wedges forming a polar network within the Cartesian arrays. Annuli and sector means were then generated for the instantaneous data, and these results were subsequently combined to produce Phase averages for various types of areal rainfall statistics. These temporally and spatially averaged results aided in the evaluation of the range performance of the various C-band radars and in the identification of range-dependent biases. They also were an integral part of the intercomparison analysis (Hudlow et al. 1979).

### 5. MERGE PROGRAMS

The instantaneous rainfall estimates for Phases I and II from the Oceanographer and Researcher radar data were merged, with the Oceanographer data being the primary source. Because of its superior range performance characteristics, the Oceanographer's radar, at the center of the B scale during Phases I and II (fig. 8), provided quantitative coverage of the entire master array (Hudlow et al. 1979). Researcher data supplemented those from the Oceanographer in the area where the Oceanographer's radar beam was often obstructed by the ship's superstructure (Richards and Hudlow 1977). The Oceanographer's ship heading was between 90° and 270° (within the southern two quadrants) for 75 percent of the observations during Phases I and II. Furthermore, when the ship's heading rotated into the northern two quadrants, it was often for a very brief period affecting only one 15-min collection sequence; therefore, the temporal

— MASTER ARRAY AND EXTENT OF OCEANOGRAPHER DATA  
- - - EXTENT OF RESEARCHER DATA



+ 8°30' N LATITUDE  
23°30' W LONGITUDE

Figure 8. Areal coverage within the master array by the Oceanographer and Researcher radars during Phases I and II.



maximization procedure applied during the hybrid processing (Richards and Hudlow 1977) usually recovered information lost in the obstructed sector in those cases.

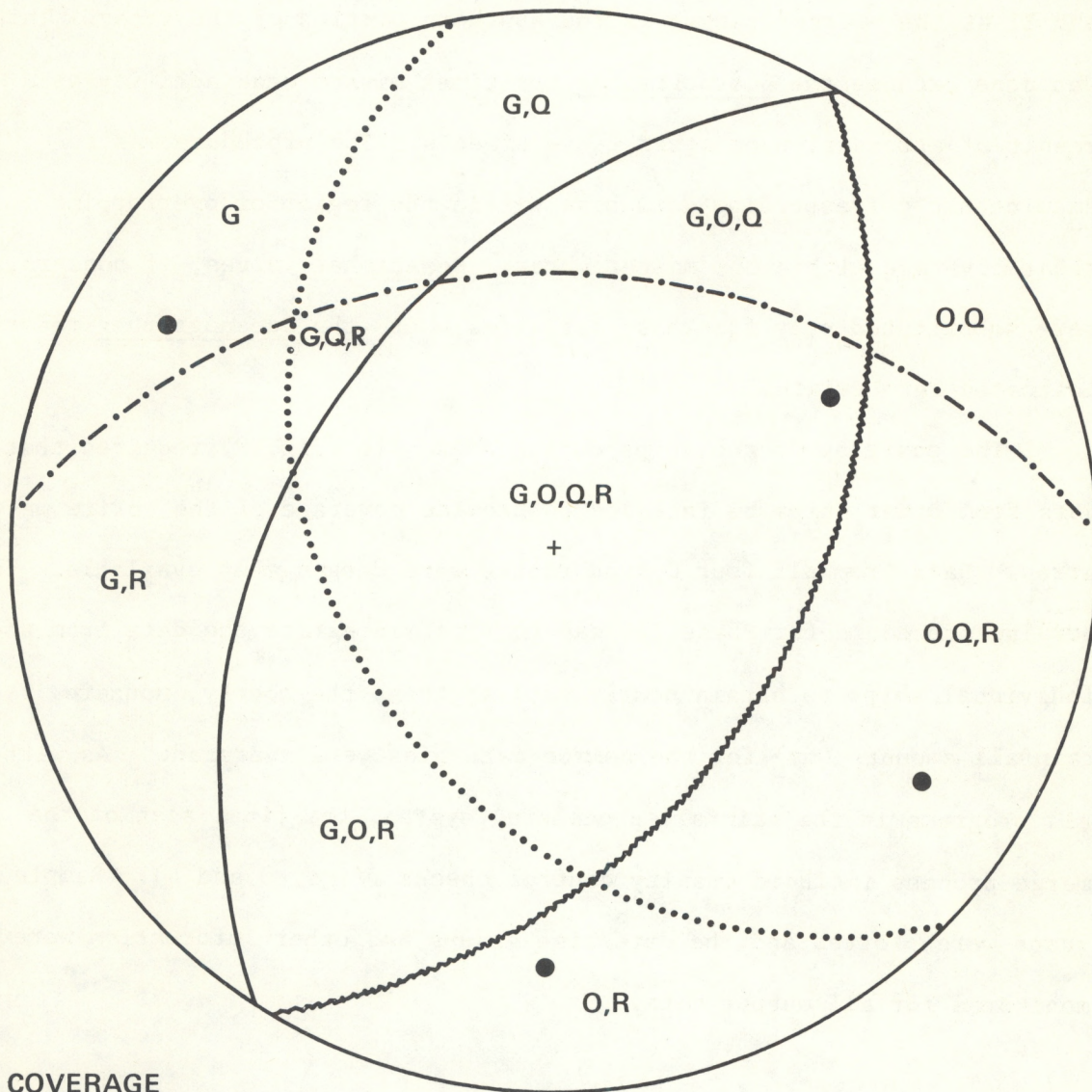
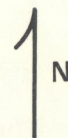
The Researcher data provided additional information during Phases I and II at the extreme ranges in the southern portion of the array. This was done because the Oceanographer sometimes missed weak activity as a result of attenuation or other range effects. The procedure was to examine the corresponding data bins within the region of overlapping radar coverage within the master array. Researcher values, if nonzero, were substituted only for those data bins where the Oceanographer radar indicated zero rainfall.

The position of the ships during Phase III (fig. 9) required that data from other ships be included to provide coverage of the entire master array. Data from all four C-band radars were merged when available. The merging procedure for Phase III was to first integrate the data from the individual ships to obtain hourly totals; then, the hourly, nonzero rainfall amounts (mm) for the common data bins were averaged.<sup>5</sup> As with all programs in the rainfall processing system, the final step of the merge process included quality control checks (figs. 3 and 4). Sample scans were plotted and the date/time groups and other information were monitored for all output data.

---

<sup>5</sup>Other merging techniques such as maximization and weighted averaging were tested, but the simple averaging procedure was chosen because it gave unbiased estimates when compared to the Phase catches from the shipboard rain gages.

- MASTER ARRAY
- ~~~~~ EXTENT OF GILLISS DATA
- EXTENT OF OCEANOGRAPHER DATA
- ..... EXTENT OF QUADRA DATA
- .-.-.-.- EXTENT OF RESEARCHER DATA



**COVERAGE**

G – GILLISS

O – OCEANOGRAPHER

Q – QUADRA

R – RESEARCHER

● LOCATION OF C – BAND  
RADAR SHIPS

+ 8° 30' N LATITUDE

23° 30' W LONGITUDE

Figure 9. Areal coverage within the master array by the four C-band radars during Phase III.

## 6. INTEGRATION PROGRAM

Total hourly rainfall accumulations were derived by integrating the instantaneous radar data using the following trapezoidal formula:

$$R_T = \frac{7.5R_5 + 15R_4 + 15R_3 + 15R_2 + 7.5R_1}{60}, \quad (10)$$

where  $R_T$  is the accumulated rainfall (mm) for the hour ending at the time  $T$  and  $R_1, R_2, R_3, R_4,$  and  $R_5$  are instantaneous rainfall rates at the times  $T, (T - 15 \text{ min}), (T - 30 \text{ min}), (T - 45 \text{ min}),$  and  $(T - 60 \text{ min}),$  respectively. There were occasions when one or more of the instantaneous scans were missing. If data were available for three or more of the five times, the integrations were always performed. If data were available for less than two of the times or if the first three or last three consecutive scans were missing, the integrations were not made. That is, integrations were still performed if two or more instantaneous scans were available and if there was no portion of the hour that was more than 30 min from an available scan. For example, when data were not available at  $(T - 45 \text{ min})$  and  $(T - 30 \text{ min}),$  the trapezoidal formula became:

$$R_T = \frac{22.5R_5 + 30R_2 + 7.5R_1}{60}. \quad (11)$$

Analogous formulas were used when data were missing for other times.

Merged instantaneous data for the Oceanographer and Researcher were integrated for Phases I and II. Data from the four C-band radars were integrated separately for Phase III. An additional multiplicative bias adjustment of 0.83 (or -0.8 dBR, expressed as an additive factor) was made to the Quadra hourly totals (Hudlow et al. 1979); the resultant hourly totals were then merged with those from the other three C-band radars (fig. 4).

Finally, the integrated data were subjected to several quality control checks (fig. 4). The date/time groups, the number of scans from each radar, and other information were printed for review. Sample scans also were plotted for visual inspection.

## 7. CONCLUDING REMARKS

The data derived with the precipitation processing system described in this paper, consisting of hourly rainfall amounts for the Cartesian network of 4-km x 4-km data bins (example shown in fig. 10), were archived on magnetic tapes and microfilm. The data set(s), together with written documentation, may be ordered from the GATE Data Catalogue (World Data Center-A 1978). In addition, coarser resolution rainfall estimates for various geometric areas and longer integration periods are included in an atlas prepared by Hudlow and Patterson (1979).

The radar estimates have been compared to available rain-gage data by Hudlow et al. (1979) and used for a variety of analyses. Although the merging process was considerably different for Phase III (sec. 5), the rainfall estimates appear to be equally accurate during all three Phases. The quality of the data are excellent, and problems

OCEANOGRAPHER RESEARCHER GILLISS QUADRA  
 NUMBER OF SCANS 4 5 5 5  
 1 SHIP 2 SHIPS 3 SHIPS 4 SHIPS  
 PERCENT OF DATA 28.9 33.4 24.7 12.7  
 RANGE MARKER INTERVAL 110 KM GRID SPACING 4 KM X 4 KM

CODE	RAINFALL (MM)	CODE	RAINFALL (MM)	CODE	RAINFALL (MM)	CODE	RAINFALL (MM)
BLANK	0.00						
1	0.01 - 0.50	5	1.46 - 2.09	9	6.10 - 8.71	■	25.41 - 36.31
2	0.50 - 0.72	6	2.09 - 2.99	10	8.71 - 12.45	■	36.31 - 51.88
3	0.72 - 1.02	7	2.99 - 4.27	11	12.45 - 17.78	■	51.88 - 74.13
4	1.02 - 1.46	8	4.27 - 6.10	12	17.78 - 25.41	■	74.13 - 105.92

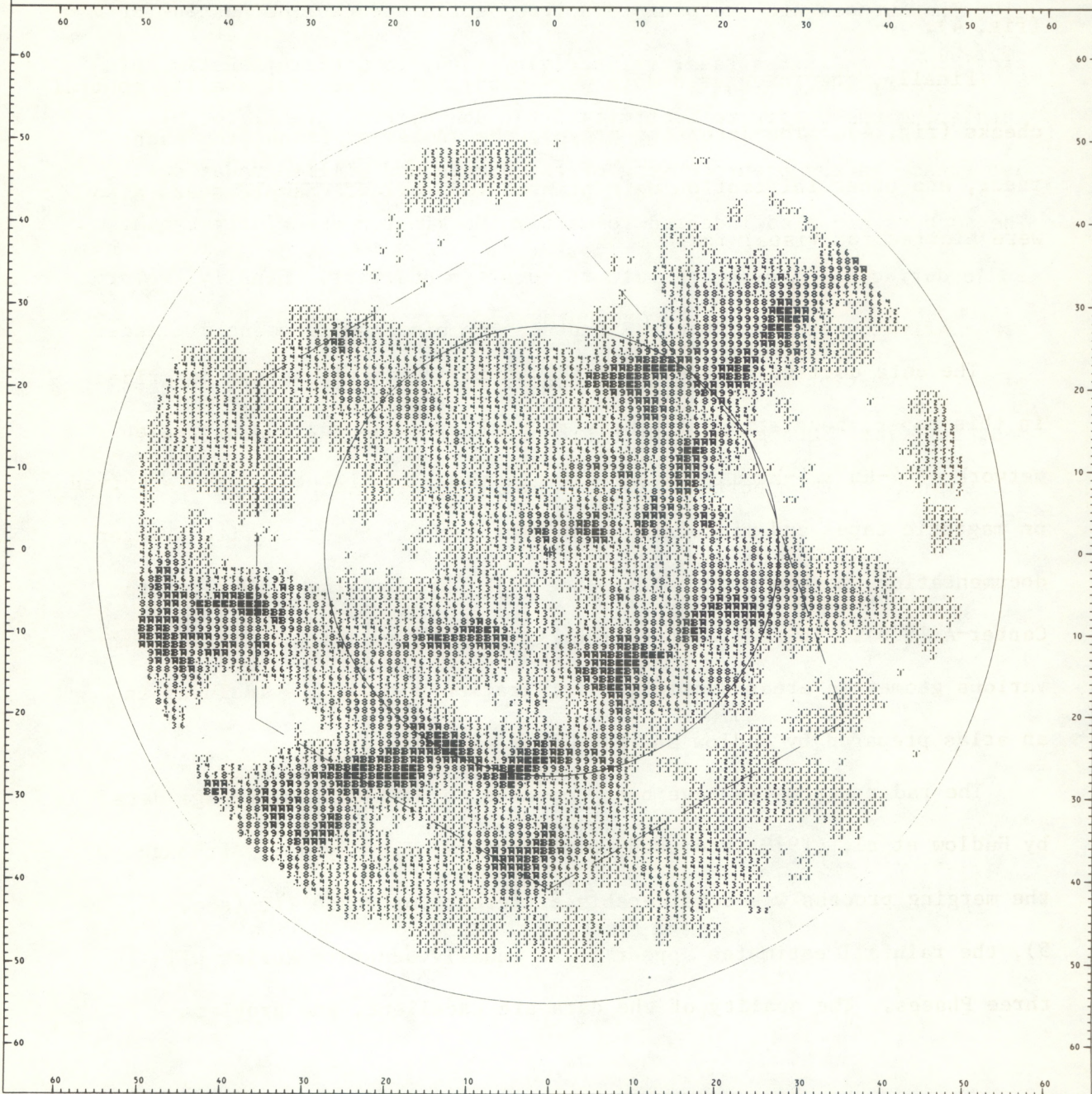


Figure 10. Sample map of hourly rainfall accumulations within the master array for the hour ending 1800 GMT on September 2.

identified in the use of the data have been very few and minor. Our experience leads us to believe that the processing system was successful and that all crucial refinements were made to improve the quality of the data set.

#### ACKNOWLEDGMENTS

The authors are grateful to Spiros Geotis and Pauline Austin for providing the Gilliss radar reflectivity data, to Geoffrey Austin for furnishing the Quadra reflectivity data, and to Rick Arkell for his assistance in the preprocessing of the Quadra and Gilliss radar data. The authors are also indebted to Carolyn Mackie for cheerfully typing and enduring the many changes to the draft manuscript. Finally, we are especially thankful to Eugene Rasmusson for his encouragement as leader of the Convection Subprogram Data Center and to all the other management staff of CEDDA and the GATE Project Office for their consistent and enthusiastic support of the GATE radar projects.

## REFERENCES

- Austin, Geoffrey L., "Documentation for GATE Quadra Radar Digital PPI Data," GATE Processed and Validated Data, GATE World Data Center A, National Climatic Center, NOAA, Federal Bldg., Asheville, N.C., 1977, 27 pp.
- Austin, Pauline, "Documentation for Gilliss Radar Cartesian Hybrid Data Set," GATE Processed and Validated Data, GATE World Data Center A, National Climatic Center, NOAA, Federal Bldg., Asheville, N.C., 1976, 79 pp.
- Austin, P. M., S. G. Geotis, J. B. Cunning, J. L. Thomas, R. I. Sax, and J. R. Gillespie, "Raindrop Size Distributions and Z-R Relationships for GATE," Paper presented at the 10 Tech. Conf. on Hurricanes and Tropical Meteor., Abstract published in the Bull. of the Amer. Meteor. Soc., Vol. 57, No. 4, 1976, p. 518.
- Geotis, Spiros G., "Some Measurements of the Attenuation of 5-CM Radiation in Rain," Preprints 16th Radar Meteor. Conf., Amer. Meteor. Soc., April 1975, pp. 63-66.
- Geotis, Spiros G., Cited in the Report of the U.S. GATE Central Program Workshop, Sponsored by NOAA and NSF, Published by National Center for Atmospheric Research, Boulder, Colo., 1977, p. 182.
- Gibble, D. (representing Bell Telephone Laboratories, Inc., Murray Hill, N.J.), "Effects of Rain on Transmission Performance of a Satellite Communication System," presented at IEEE International Convention, New York, N.Y., March 1964, (Abstract only available in Conference Proceedings.)
- Greene, Douglas R., "Numerical Techniques for the Analysis of Digital Radar Data with Applications to Meteorology and Hydrology," Ph.D. Dissertation, Texas A&M University, College Sta., Tex., 1971, 125 pp.
- Hildebrand, Peter H., "Iterative Correction for Attenuation of 5 cm Radar in Rain," J. Appl. Meteor., Vol. 17, No. 4, 1978, pp. 508-514.
- Hudlow, Michael D., "Collection and Handling of GATE Shipboard Radar Data," Preprints 16th Radar Meteor. Conf., Amer. Meteor. Soc., April 1975, pp. 186-193.
- Hudlow, Michael D., "Documentation for GATE NOAA Radar Hybrid Data," GATE Processed and Validated Data, GATE World Data Center A, National Climatic Center, NOAA, Federal Bldg., Asheville, N.C., 1976, 31 pp.
- Hudlow, Michael D., Peter J. Pytlowany, and Frank D. Marks, "Objective Analysis of GATE Collocated Radar and Rain Gage Data," Preprints 17th Radar Meteor. Conf., Amer. Meteor. Soc., Oct. 1976, pp. 414-421.

- Hudlow, Michael D., and Richard E. Arkell, "Effect of Temporal and Spatial Sampling Errors and Z-R Variability on Accuracy of GATE Radar Rainfall Estimates," Preprints 18th Radar Meteor. Conf., Amer. Meteor. Soc., Mar. 1978, pp. 342-349.
- Hudlow, M., R. Arkell, V. Patterson, P. Pytlowany, F. Richards, and S. Geotis, "Calibration and Intercomparison of the GATE C-Band Radars," NOAA Tech. Report EDIS 31, Center for Environmental Assessment Services, NOAA, U.S. Dept. of Commerce, Washington, D.C., in preparation, 1979.
- Hudlow, Michael D., and Vernon L. Patterson, "GATE Radar Rainfall Atlas," NOAA Special Report, Center for Environmental Assessment Services, NOAA, U.S. Dept. of Commerce, Washington, D.C., 1979.
- Jallickee, J. B., J. S. Ching, and J. A. Almazan, "Objective Analysis of IFYGL Surface Meteorological Data," Proc. 17th Conf. Great Lakes Res., Internat. Assoc. Great Lakes Res., Toronto, Ont., 1974, pp. 733-750.
- Richards, Frank, and Michael D. Hudlow, "Use and Abuse of the GATE Digital Radar Data," 11th Tech. Conf. on Hurricanes and Tropical Meteor., Amer. Meteor. Soc., Dec. 1977, pp. 216-223.
- Seguin, Ward R., and Raymond Crayton, "Documentation for the U.S. GATE B-Scale Navigation Data," GATE Processed and Validated Data, GATE World Data Center A, National Climatic Center, NOAA, Federal Bldg., Asheville, N.C., 1975, 25 pp.
- World Data Center - A, GATE Data Catalogue, National Climatic Center, NOAA, Federal Bldg., Asheville, N.C., 1978, pp. 4.36.02.104 and 4.36.02.105.



(Continued from inside front cover)

- EDSTM 15 Improved Estimates of Winds at Standard Heights Generated From Winds Recorded at Standard Pressure Levels. Harold L. Crutcher, Russell F. Lee, and H. B. Harshbarger, March 1970. (PB-192-904)
- EDSTM 16 Georgia Tornadoes. Horace S. Carter, July 1970. (PB-194-209)
- EDSTM 17 Ground Rainfall Data for the 1968 Florida Cloud Seeding Experiment. B. G. Holzman and Marcella Thom, August 1970.

NOAA Technical Memorandums

- EDS 18 The Effect of Atmospheric Aerosol on Climate With Special Reference to Surface Temperature. J. Murray Mitchell, Jr., November 1970. (COM-71-00341)
- EDS 19 Terrain and Climate. Robert L. Schloemer, April 1971.
- EDS 20 Drought Bibliography. Wayne C. Palmer and Lyle M. Denny, June 1971. (COM-71-00937)
- EDS 21 Bibliography of the Urban Modification of the Atmospheric and Hydrologic Environment. John F. Griffiths and M. Joan Griffiths, February 1974. (COM-74-10962/AS)
- EDS 22 Probability of Sequences of Wet and Dry Days for Tennessee. John M. Safley, Jr., Henry A. Fribourg, John V. Vaiksnoras, and Rodney H. Strand, September 1974. (COM-75-10650)
- EDS 23 Probability of Low and High Temperatures in Tennessee. Henry A. Fribourg and Dewayne L. Ingram, March 1978. (PB-280-741)
- EDS 24 Heating and Cooling Degree Days for Tennessee. Dewayne L. Ingram and Henry A. Fribourg, March 1978. (PB-280-740)
- EDIS 25 Cost-Benefit Analysis of Selected Environmental Data Service Programs. Robert C. Anderson and Norman F. Meade, January 1979.

# NOAA SCIENTIFIC AND TECHNICAL PUBLICATIONS

*The National Oceanic and Atmospheric Administration* was established as part of the Department of Commerce on October 3, 1970. The mission responsibilities of NOAA are to assess the socioeconomic impact of natural and technological changes in the environment and to monitor and predict the state of the solid Earth, the oceans and their living resources, the atmosphere, and the space environment of the Earth.

The major components of NOAA regularly produce various types of scientific and technical information in the following kinds of publications:

**PROFESSIONAL PAPERS** — Important definitive research results, major techniques, and special investigations.

**CONTRACT AND GRANT REPORTS** — Reports prepared by contractors or grantees under NOAA sponsorship.

**ATLAS** — Presentation of analyzed data generally in the form of maps showing distribution of rainfall, chemical and physical conditions of oceans and atmosphere, distribution of fishes and marine mammals, ionospheric conditions, etc.

**TECHNICAL SERVICE PUBLICATIONS** — Reports containing data, observations, instructions, etc. A partial listing includes data serials; prediction and outlook periodicals; technical manuals, training papers, planning reports, and information serials; and miscellaneous technical publications.

**TECHNICAL REPORTS** — Journal quality with extensive details, mathematical developments, or data listings.

**TECHNICAL MEMORANDUMS** — Reports of preliminary, partial, or negative research or technology results, interim instructions, and the like.



*Information on availability of NOAA publications can be obtained from:*

**ENVIRONMENTAL SCIENCE INFORMATION CENTER (D822)  
ENVIRONMENTAL DATA AND INFORMATION SERVICE  
NATIONAL OCEANIC AND ATMOSPHERIC ADMINISTRATION  
U.S. DEPARTMENT OF COMMERCE**

**6009 Executive Boulevard  
Rockville, MD 20852**

NOAA--S/T 78-442

